

SIMULATIONS AND ANALYSIS OF GRAVITATIONALLY REDSHIFTED KERR BLACK HOLE ACCRETION DISCS

Benjamin Puzantian^{1, a)}, Steve Desjardins², and Christian Giguault¹

¹ *Department of Physics, University of Ottawa, Ottawa ON Canada*

² *Department of Mathematics and Statistics, University of Ottawa, Ottawa ON Canada*

^{a)} Corresponding author: bpuza021@uottawa.ca

Abstract. The Kerr black hole rotates with two parameters: mass M and angular momentum a and is characterized by the Kerr metric (Taylor and Wheeler 2000). Hence, a binary pair of a black hole and a star can create an accretion disc. A Kerr ray tracer algorithm was used to simulate accretion discs in the Seyfert-1 galaxy. The power law observed flux of relativistic emission lines, and Kerr Fourier image analysis methods were applied to the simulated discs. Simulated image characteristics were analyzed. Power laws were fitted to the simulated data of the Mrk110 accretion disc. Lastly, the simulated images were transformed into Fourier space and characteristics were discussed.

INTRODUCTION

Accreting black holes are of particular interest in modern cosmology. An accreting black hole has a disc of matter pseudo-orbiting the black hole. Systems such as active galactic nuclei (AGN) and supermassive black holes are accreting systems that yield characteristic information about the black holes. The AGN considered in this paper are Seyfert-1 galaxies that emit luminosity characterized spectral lines. (Carroll and Ostlie 1996).

Emissivity theory is a method of finding the emission lines of an accreting black hole. By theoretically simulating accreting black holes, a best fit power law can be produced that describes the relationship between the redshift as a function of radius along the accretion disc. Hence, the effects of gravitational redshift in the neighbourhood of a Kerr black hole can be examined. Furthermore, inclinations, mass and best-fit slopes can be extrapolated and interpolated from these best-fit power laws.

From Fourier theory, images in the spatial domain can be transformed into the Fourier domain. Thus, frequency intensities in the transformed images can be seen more distinctly and discs with higher inclinations should show a greater degree of structure.

Kerr Ray Tracer

Light rays emitted from the accretion disc near the black hole travel on a null geodesic. The Kerr ray tracer maps the emitted points of light rays in the equatorial plane of a Kerr black hole to points on the observer's plane.

The redshift factor g is a factor that measures the distribution over the accretion disk and is defined as

$$g \equiv \frac{v_{obs}}{v_{em}} = \frac{1}{1+z} \quad (1)$$

where $c = 1$, v_{obs} is the observed photon momentum, v_{em} is the emitted photon momenta, and z is the redshift.

The MATLAB computational program based on Chen et al.'s KERTAP was used. The KERTAP uses a GUI and then prompts the user for parameters of an accretion disc around a typical black hole, the image resolution, and the number of parallel works used in the program's computation. At termination, the GUI produces a redshifted image of the accretion disc (i.e. FIG. 1 and FIG. 2). Due to the emission region's close proximity to the black hole, the standard linearized gravitational lens theory cannot be applied. Thus, a backward ray-trace is required. This is done by dividing the solid angle of the beam into a uniform grid of pixels (Chen et al., 2015). Therefore, in the computation of the observed flux, the pixels are numerically computed as

$$F_{\nu_0} = \int g^3(\hat{n}) I_{\nu_e}^{source}(x^a(\hat{n}), p_a(\hat{n})) d\Omega_0 \quad (2)$$

where ν_e is the source frequency, I_ν is the radiated energy field that is a conserved quantity along the light path, \hat{n} is the three-dimensional photon direction at the observer, and $(x^a(\hat{n}), p_a(\hat{n}))$ is the photon's position and momentum at the emitter.

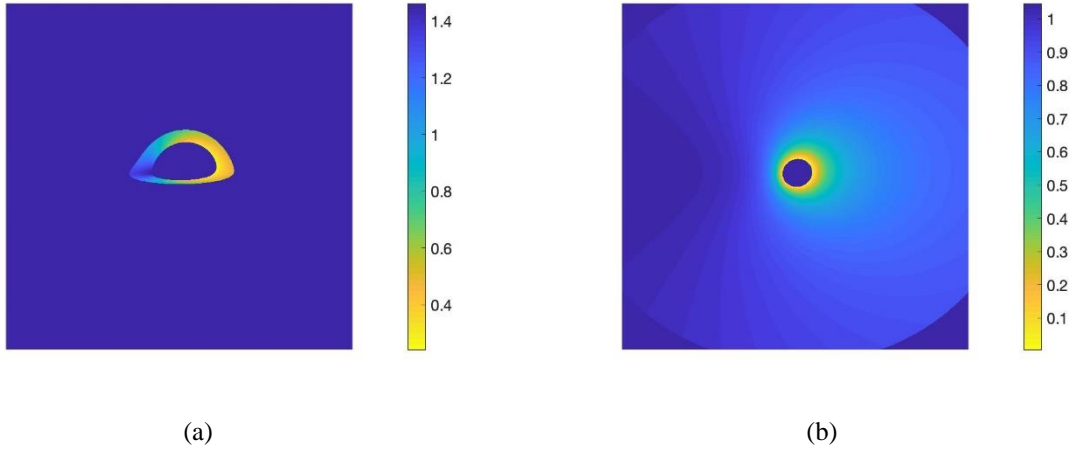


FIGURE 1. (a) Simulated Kerr accretion disk of radius $6.2r_g$ around a black hole of mass $6.2 M$, angular momentum $a=0.8$, inclined at $i = 80^\circ$, and an observational radius of $1 \times 10^6 r_g$. The scale indicates redshift factor, g . (b) Simulated extreme Kerr accretion disk of $31.015r_g$ around a black hole of mass $31.995 M$ with angular momentum of $a=0.999999$, inclined at $i = 30^\circ$, and an observational radius of $1 \times 10^6 r_g$. The scale indicates redshift factor, g .

Figure 1a is a simulated highly inclined, fast rotating accretion disc. The accretion disc is beamed, (i.e. $g > 1$), on the lower left side (indicated by the dark blue). On the right side of the accretion disc, the region close to and around the horizon, that is, the yellow part of the right side, is strongly redshifted, i.e. ($g < 1$). Hence, for highly inclined rotating discs the blue beaming part (i.e. the dark blue in FIG. 1a) approaching the observer is significantly strong and can be seen intensely. Therefore, if an observer were to look at a highly-inclined standard accretion disc of a cosmic black hole, a sudden step in gravitational redshift is a distinct and real observable feature. The anti-symmetry of the figure is due to the g -factor changing from high values in the beaming feature to smaller values. It should be noted that the colours in the FIG. 1a and FIG. 1b do not have any relation to the continuum spectra of AGNs nor Doppler effects, but rather is a product of simulation scaling.

Figure 1b is an extreme Kerr black hole in a typical Seyfert-1 galaxy. The accretion disc has a blue beam wing approaching the left side, that is the triangular-shaped blue region seen on the left side of FIG. 1b. This wing represents a region where the redshift factor is greater than 1; though, the gravitational redshift becomes sufficiently greater as the event horizon is approached, since the redshift factor approaches 0 until g vanishes at the event horizon.

Power Laws

A simple power law can be used to find core redshift values for accretion discs, as simulated in the Seyfert-1 galaxy. A power law equation (Müller et al. 2006) describing the core redshift values is

$$z = pr^s \quad (3)$$

where r is the radial range of the accretion disc, p is the projection parameter and s is the slope at an inclination i .

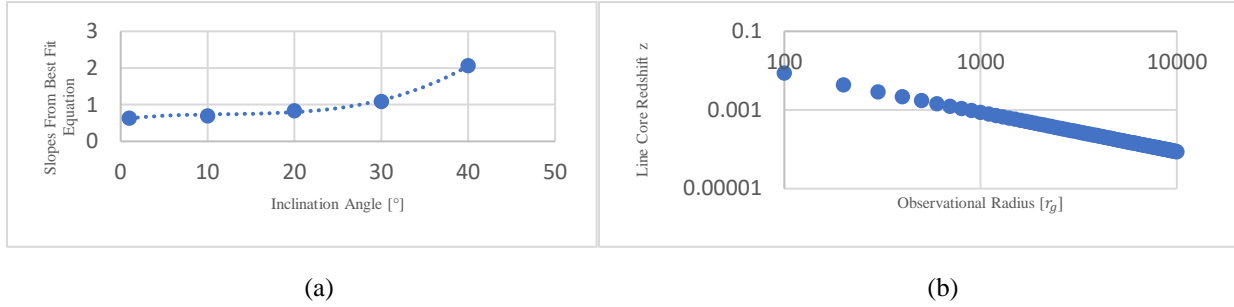


FIGURE 2. (a) Best fit slopes versus inclination angle. (b) Linearized line core redshift for the $p=0.88$ Mrk110 accretion disc.

The Mrk 110 accretion disc from the Seyfert-1 galaxy was simulated for a radial accretion disc at an inclination of $i = 30^\circ$ in the Thorne limit of $a = 0.998$, that is, a theoretical limit found by Thorne (1974) to be the maximum angular momentum of a Kerr black hole, $a = J/m^*$ and m^* is the mass of a black hole such that $m^* = Gm/c^2$. The line core redshifts were computed using equation 3 for different inclinations of the Mrk110 accretion disc from $I = 1, 10, 20, 30,$ and 40 , a theoretical Kerr power law slope of $s = -1$.

When plotting the slopes of the best fit equations from the line core redshift plots of Mrk110 accretion discs against inclination angle, a third-order polynomial provided the best fit (Fig. 2a).

Figure 2b shows the reciprocal line core redshifts for the inclinations aforesaid plotted against observational distance (1 to 10000). The reciprocal was taken to linearize the line core redshifts such that a linear best fit trendline can be created. It was found that points were spread within 5×10^{-3} to 10^{-5} range. The best fit slope for $p = 0.88$ was found to be -1.1364 which is lower than Muller et al.'s (2006) slope of -1.002 ± 0.005 .

Kerr Fourier Image Analysis

Simulation images produced for the Mrk110 accretion disc from the Seyfert-1 galaxy (such as Fig. 1) were Fourier transformed using the Fourier image transform and log-Fourier image transform.

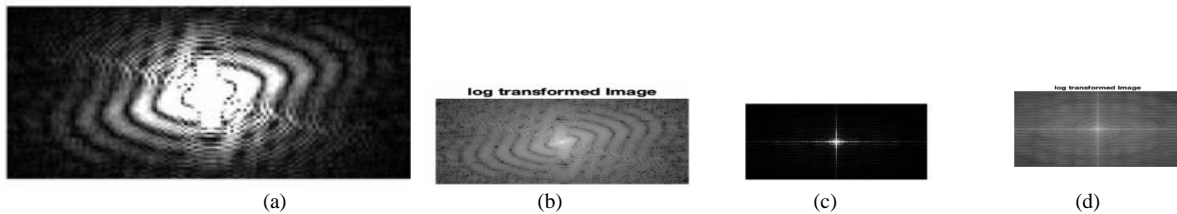


FIGURE 3. (a) Normalized Fourier transformation accretion disc of radius $6.2r_g$ around a black hole of mass $6.2 M$, with angular momentum $a=0.8$, inclined at $i = 80^\circ$, and an observational radius of $1 \times 10^6 r_g$. (b) Log Fourier transformation of the same disc. (c) Normalized Fourier transformation of an accretion disc of radius $31.015r_g$ around a $31.995 M$ black hole with an angular momentum of $a=0.999999$, $i = 30^\circ$, and observational radius of $1 \times 10^6 r_g$. (d) The log-transform of (c).

It was found that higher inclination angles (such as in Fig. 3a) were highly structured in Fourier space while in lower inclination angles (such as Fig. 3c) the images were less structured in Fourier space. However, in all cases, the images in Fourier space show the sites of the gravitational redshifts more distinctly. The circular rings in Fig. 3d are an indication of a source of discontinuity on the images in Fourier space.

CONCLUSIONS

The highly inclined rotating disc was found to have a blue beaming part approaching the observer far away from the event horizon. Extreme Kerr black holes were found to have a blue beaming wing in the shape of a triangular-like pie that represents a region where $g > 1$. For the Mrk110 accretion disc in the Seyfert-1 galaxy, a best fit slope for $p =$

0.88 was found to be -1.1364 , which is lower than the well-established slope of -1.002 ± 0.005 . This is due to the data points being mainly on the right side of the linearized figures which effects the slope in the least-square fit.

When the least-square fits were plotted against inclination angle, the data conformed to a pseudo-polynomial that best fits to a cubic polynomial. The plot is an empirical model that is useful for interpolation and extrapolation. It was found that for accretion discs with higher inclinations, there was a higher concentration of structure in Fourier space; while for lower inclinations there was a lower concentration of structure in Fourier space.

In conclusion, we confirmed the Muller et al. analysis on Mrk110 and other accretion discs (2004, 2006) and expanded on them. Moreover, further experimental analysis can be done to interpolate and extrapolate gravitational redshift values from the pseudo-polynomial plot. Also, further Fourier analysis on the transformed images could show more physical characteristic information about the accretion disc.

ACKNOWLEDGMENTS

I would like to thank Dr. Steven J. Desjardins for all of his inspiring discussions and support. I would also like to thank Dr. Christian Gigault for all of his help. I have personally and professionally benefited from all of their support. Special thanks the anonymous reviewer for their feedback.

REFERENCES

1. B. Carroll and D. Ostlie. "Modern Astrophysics", Ch. 26: Active Galaxies, Addison-Wesley (1996).
2. B. Chen, R. Kantowski, X. Dai, E. Baron, and P. Maddumage, Algorithms and Programs for Strong Gravitational Lensing in Kerr Space-Time Including Polarization, *Astrophys. J. Suppl. Ser.* **218:4**, 1-11 (2015).
3. W. Kollatschny, Accretion Disk Wind in the AGN Broad-Line Region: Spectroscopically Resolved Line Profiles Variations in Mrk 110, *Astronomy and Astrophysics* **407**, 461-472 (2003).
4. A. Muller and M. Cammenzind, Relativistic Emission Lines from Accreting Black Holes: The Effect of Disk Truncation on Line Profiles, *Astronomy and Astrophysics* **413**, No 4, 861-878 (2004).
5. A. Muller, The Onset of General Relativity: Gravitationally Redshifted Emission Lines, *Astron. Nachr, AN* 327, No.10. (2006).
6. A. Muller and M. Wold, On the Signatures of Gravitational Redshift: The Onset of Relativistic Emission Lines, *Astronomy and Astrophysics* **457**, 438-492 (2006).
7. B. Puzantian, "Simulations and Analysis of Gravitational Redshift of a Kerr Black Hole Accretion Disc," BSc Honour Research Project, University of Ottawa, Ottawa (2019).
8. E. Taylor and J.A. Wheeler, "Project F: The Spinning Black Hole". *Exploring Black Holes*, Addison Wesley Longman, (2000).
9. K.S. Thorne, Disk-Accretion onto a Black Hole. II. Evolution of the Hole, *Astrophys. J.*, **191**, 429 (1974).